

## Deep seawater inherent optical properties in the Southern Ionian Sea

G. Riccobene <sup>a,\*</sup>, A. Capone <sup>i</sup>, S. Aiello <sup>c</sup>, M. Ambriola <sup>d</sup>,  
 F. Ameli <sup>i</sup>, I. Amore <sup>a,j</sup>, M. Anghinolfi <sup>f</sup>, A. Anzalone <sup>a</sup>,  
 C. Avanzini <sup>h</sup>, G. Barbarino <sup>g</sup>, E. Barbarito <sup>d</sup>, M. Battaglieri <sup>f</sup>,  
 R. Bellotti <sup>d</sup>, N. Beverini <sup>h</sup>, M. Bonori <sup>i</sup>, B. Bouhadeh <sup>h</sup>,  
 M. Brescia <sup>g,k</sup>, G. Cacopardo <sup>a</sup>, F. Cafagna <sup>d</sup>, L. Caponetto <sup>c</sup>,  
 E. Castorina <sup>h</sup>, A. Ceres <sup>d</sup>, T. Chiarusi <sup>i</sup>, M. Circella <sup>d</sup>,  
 R. Cocimano <sup>a</sup>, R. Coniglione <sup>a</sup>, M. Cordelli <sup>b</sup>, M. Costa <sup>a</sup>,  
 S. Cuneo <sup>f</sup>, A. D'Amico <sup>a</sup>, G. De Bonis <sup>i</sup>, C. De Marzo <sup>d,1</sup>,  
 G. De Rosa <sup>g</sup>, R. De Vita <sup>f</sup>, C. Distefano <sup>a</sup>, E. Falchini <sup>h</sup>,  
 C. Fiorello <sup>d</sup>, V. Flaminio <sup>h</sup>, K. Fratini <sup>f</sup>, A. Gabrielli <sup>e</sup>,  
 S. Galeotti <sup>h</sup>, E. Gandolfi <sup>e</sup>, A. Grimaldi <sup>c</sup>, R. Habel <sup>b</sup>,  
 E. Leonora <sup>c,j</sup>, A. Lonardo <sup>i</sup>, G. Longo <sup>g</sup>, D. Lo Presti <sup>c,j</sup>,  
 F. Lucarelli <sup>i</sup>, E. Maccioni <sup>h</sup>, A. Margiotta <sup>e</sup>, A. Martini <sup>b</sup>,  
 R. Masullo <sup>i</sup>, R. Megna <sup>d</sup>, E. Migneco <sup>a,j</sup>, M. Mongelli <sup>d</sup>,  
 M. Morganti <sup>h</sup>, T. Montaruli <sup>l,4</sup>, M. Musumeci <sup>a</sup>, C.A. Nicolau <sup>i</sup>,  
 A. Orlando <sup>a</sup>, M. Osipenko <sup>f</sup>, G. Osteria <sup>g</sup>, R. Papaleo <sup>a</sup>,  
 V. Pappalardo <sup>a</sup>, C. Petta <sup>c,j</sup>, P. Piattelli <sup>a</sup>, F. Raffaelli <sup>h</sup>,  
 G. Raia <sup>a</sup>, N. Randazzo <sup>c</sup>, S. Reito <sup>c</sup>, G. Ricco <sup>f</sup>, M. Ripani <sup>f</sup>,  
 A. Rovelli <sup>a</sup>, M. Ruppi <sup>d</sup>, G.V. Russo <sup>c,j</sup>, S. Russo <sup>g</sup>, S. Russo <sup>a,2</sup>,  
 P. Sapienza <sup>a</sup>, M. Sedita <sup>a</sup>, J-P. Schuller <sup>i,3</sup>, E. Shirokov <sup>f</sup>,  
 F. Simeone <sup>i</sup>, V. Sipala <sup>c,j</sup>, M. Spurio <sup>e</sup>, M. Taiuti <sup>f</sup>, G. Terreni <sup>h</sup>,  
 L. Trasatti <sup>b</sup>, S. Urso <sup>c</sup>, V. Valente <sup>b</sup>, P. Vicini <sup>i</sup>,

<sup>a</sup>Laboratori Nazionali del Sud INFN, Via S.Sofia 62, 95123, Catania, Italy

<sup>b</sup>Laboratori Nazionali di Frascati INFN, Via Enrico Fermi 40, 00044, Frascati (RM), Italy

<sup>c</sup>INFN Sezione Catania, Via S.Sofia 64, 95123, Catania, Italy

<sup>d</sup>INFN Sezione Bari and Dipartimento Interateneo di Fisica Università di Bari, Via E. Orabona 4, 70126, Bari, Italy

<sup>e</sup>INFN Sezione Bologna and Dipartimento di Fisica Università di Bologna, V.le Bertini Pichat 6-2, 40127, Bologna, Italy

<sup>f</sup>INFN Sezione Genova and Dipartimento di Fisica Università di Genova, Via

*Dodecaneso 33, 16146, Genova, Italy*

<sup>g</sup>*INFN Sezione Napoli and Dipartimento di Scienze Fisiche Università di Napoli,  
Via Cintia, 80126, Napoli, Italy*

<sup>h</sup>*INFN Sezione Pisa and Dipartimento di Fisica Università di Pisa, Polo  
Fibonacci, Largo Bruno Pontecorvo 3, 56127, Pisa, Italy*

<sup>i</sup>*INFN Sezione Roma 1 and Dipartimento di Fisica Università di Roma "La  
Sapienza", P.le A. Moro 2, 00185, Roma, Italy*

<sup>j</sup>*Dipartimento di Fisica and Astronomia Università di Catania, Via S.Sofia 64,  
95123, Catania, Italy*

<sup>k</sup>*INAF Osservatorio Astronomico di Capodimonte, Salita Moiariello 16, 80131,  
Napoli, Italy*

<sup>l</sup>*University of Wisconsin, Department of Physics, 53711, Madison, WI, USA*

---

## Abstract

The NEMO (NEutrino Mediterranean Observatory) Collaboration has been carrying out since 1998 an evaluation programme of deep sea sites suitable for the construction of the future Mediterranean km<sup>3</sup> Čerenkov neutrino telescope. We investigated the seawater optical and oceanographic properties of several deep sea marine areas close to the Italian Coast. Inherent optical properties (light absorption and attenuation coefficients) have been measured as a function of depth using an experimental apparatus equipped with standard oceanographic probes and the commercial transmissometer AC9 manufactured by WETLabs. This paper reports on the visible light absorption and attenuation coefficients measured in deep seawater of a marine region located in the Southern Ionian Sea, 60÷100 km SE of Capo Passero (Sicily). Data show that blue light absorption coefficient is about 0.015 m<sup>-1</sup> (corresponding to an absorption length of 67 m) close to the one of optically pure water and it does not show seasonal variation.

*Key words:* underwater Čerenkov neutrino telescope, deep seawater optical properties, light attenuation, light absorption  
*PACS:* 95.55.Vj, 29.40.Ka, 92.10.Pt, 07.88.+y

---

\* Fax: +39 095 542 398

*Email address:* riccobene@lns.infn.it (G. Riccobene).

<sup>1</sup> Deceased

<sup>2</sup> Present address: Istituto Centrale per la Ricerca Scientifica e Tecnologica Applicata al Mare, via Casalotti 300, 00166, Roma, Italy

<sup>3</sup> Present address: DAPNIA/SPP Bt 141 CEN Saclay, 91191 Gif-sur-Yvette, France

<sup>4</sup> On leave of absence Dipartimento Interateneo di Fisica Università di Bari, Via E. Orabona 4, 70126, Bari, Italy

## 1 Introduction

The construction of  $\text{km}^3$ -scale high energy neutrino telescopes will complement and extend the field of high energy astrophysics allowing the identification of the highest energy cosmic ray sources. The search for astronomical sources of high energy cosmic rays is possible with particles that reach un-deflected the detectors. The observational horizon of high energy cosmic gamma rays and nuclei from ground based detectors is limited to few tens of Mpc by the interaction with cosmic matter and radiation: this should imply the well known GZK cutoff (1; 2) in the energy distribution of ultra high energy extragalactic cosmic rays. On the contrary, the low cross section of weak interaction allows neutrinos to reach the Earth un-deflected from the farthestmost regions of the Universe. Active Galactic Nuclei (3), Galactic Supernova Remnants (4), Microquasars (5) and Gamma Ray Bursters (6) are some of the most promising candidate of high energy muon-neutrino sources. On the basis of high energy neutrino fluxes, calculated using astrophysical models, neutrino detectors with an effective area of  $\simeq 1 \text{ km}^2$  will be able to collect, in one year, a statistically significant number of events from point-like astrophysical neutrino sources.

Underwater Čerenkov telescopes detect high energy neutrinos indirectly, tracking the Čerenkov light wavefront radiated, in seawater or in ice, by charged leptons originated in Charged Current neutrino interactions. Seawater, therefore, acts as a neutrino target and as a Čerenkov radiator. An undersea location at a depth of more than 3000 m provides an effective shielding for atmospheric muons background and allows the construction of such detectors, usually referred as *Neutrino Telescopes* (7). Two smaller scale neutrino detectors, AMANDA and BAIKAL, have already collected and reported candidate neutrino events (8; 9). AMANDA is located in the South Pole icecap (10) at a depth between 1400 and 2400 m. The present size is relatively small, about  $25000 \text{ m}^2$  for TeV muons, compared to IceCube (11), the future  $\text{km}^3$  detector now under construction. BAIKAL NT-200, the pioneer underwater detector, is deployed in the Siberian Lake Baikal at about 1000 m depth and has a detection area close to  $10^4 \text{ m}^2$  for TeV muons (12).

In the Northern Hemisphere, the Mediterranean Sea offers several areas with depths greater than 3000 m; few are close to scientific and logistic infrastructures and offer optimal conditions to install an underwater  $\text{km}^3$  neutrino telescope. The future IceCube and the Mediterranean  $\text{km}^3$  will complement each other providing a global  $4\pi$  observation of the sky. The long light absorption length of the Antarctic ice is expected to allow good energy resolution, the long light effective scattering length of the Mediterranean seawater should also allow excellent angular resolution. Three collaborations, NESTOR (13), ANTARES (14) and NEMO (15), are presently active in the Mediterranean Sea. NESTOR proposes the installation of a Čerenkov detector, with a tower-

shaped geometry, moored a few nautical miles off the south-west tip of the Peloponnese (Greece), at about 4000 m depth. ANTARES is building a detector in the vicinity of Toulon (France) at  $\simeq 2450$  m depth to possibly detect astrophysical neutrinos and to demonstrate the feasibility of a  $\text{km}^3$ -scale underwater neutrino telescope.

The NEMO Collaboration is active in the design and tests for the Mediterranean  $\text{km}^3$  neutrino telescope. After a long period of *R&D* activity, at present the collaboration is ready to install a prototype station (NEMO *phase 1*) at 2000 m depth, 25 km offshore the town of Catania, in Sicily (*Test Site* in Figure 1). Since 1998 we have performed more than 25 oceanographic campaigns in the Central Mediterranean Sea in order to characterize and eventually seek an optimal submarine site for the installation of the Mediterranean  $\text{km}^3$  (16). Three areas close to the Italian Coast have been compared, on the basis of two requirements: depth  $> 3000$  m and distance from shore  $< 100$  km. Two of these sites are trenches located in the Southern Tyrrhenian Sea close to the Alicudi and Ustica Islands (at depth  $\simeq 3500$  m). Measurements of deep seawater optical properties were performed by the NEMO Collaboration in these sites and results were published (17). The third site is a submarine plateau, whose average depth is  $\simeq 3500$  m, located at a distance of  $40\div 100$  km South East of Capo Passero, Sicily (see Figure 1). In this paper we report on deep seawater optical properties (absorption and attenuation coefficients) measured in the *Capo Passero* marine region during a period extending from December 1999 to July 2003. The results refer to two sites located  $\simeq 60$  km ( $36^\circ 30' \text{N}, 15^\circ 50' \text{E}$ ) and  $\simeq 80$  km ( $36^\circ 25' \text{N}, 16^\circ 00' \text{E}$ ) offshore *Capo Passero*, hereafter indicated respectively as *KM3* and *KM4*. The programme of characterisation of deep seawater in *Capo Passero* site, carried out by the NEMO Collaboration, includes also long term measurements of optical background (due to bioluminescence and  $^{40}\text{K}$  radioactive decays), water temperature and salinity, deep sea currents, sedimentation rate and bio-fouling. The results of this work are presented elsewhere (18) and will be published soon.

## 2 Measurements of water optical properties with the AC9

The propagation of light in water is quantified, for a given wavelength  $\lambda$ , by the water Inherent Optical Properties (IOP): the absorption  $a(\lambda)$ , scattering  $b(\lambda)$  and attenuation  $c(\lambda) = a(\lambda) + b(\lambda)$  coefficients. The light propagation in water can be described by the laws:

$$\begin{aligned} I_a(x, \lambda) &= I_0(\lambda)e^{-x \cdot a(\lambda)} \\ I_b(x, \lambda) &= I_0(\lambda)e^{-x \cdot b(\lambda)} \\ I_c(x, \lambda) &= I_0(\lambda)e^{-x \cdot c(\lambda)} \end{aligned}$$

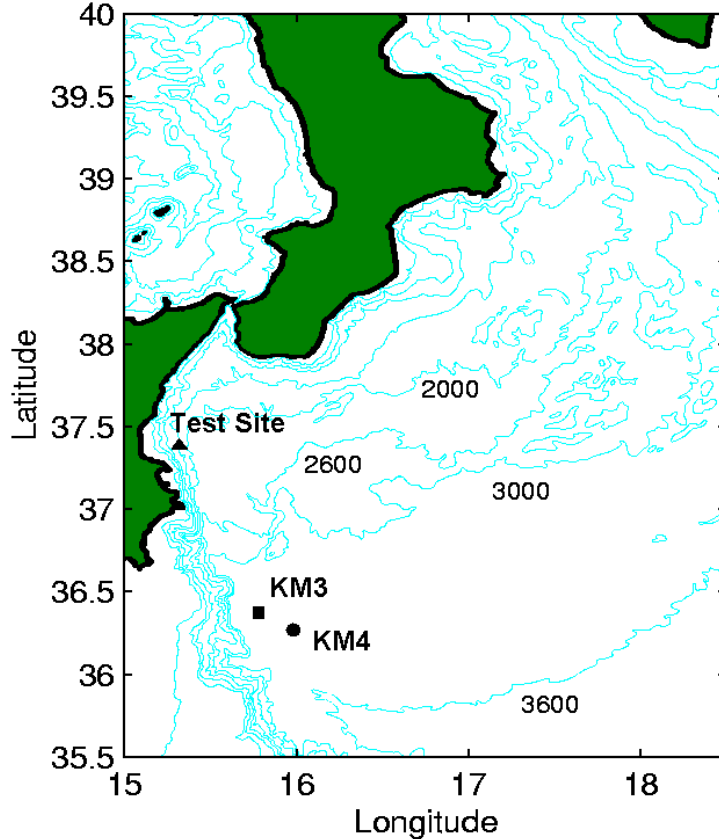


Fig. 1. Bathymetric chart of the *Capo Passero* region. The location of the *KM3* (square) and *KM4* (circle) sites and of the NEMO Phase 1 *Test Site* (triangle) is shown. The seabed depth is about 3400 m for the *Capo Passero* sites and 2000 m for the *Test Site*.

where  $x$  is the optical path traversed by the light and  $I_0(\lambda)$  is the source intensity. A complete description of light scattering in water would require the knowledge of another IOP, i.e. the scattering angular distribution, or volume scattering function,  $\tilde{\beta}(\vartheta, \lambda)$ . Integrating this function over the diffusion angle  $\vartheta$  one gets  $b(\lambda)$ . In this paper we shall report on measurements of  $c(\lambda)$  and  $a(\lambda)$  for visible light wavelengths performed with a commercial transmissometer, the AC9 manufactured by WETLabs (19). It is worth to mention that the AC9 performs measurements of the attenuation coefficient in a collimated geometry: the angular acceptance of the  $c(\lambda)$  channel is  $\simeq 0.7^\circ$ . The reported values of  $c(\lambda)$  are not directly comparable with the results often reported by other authors that concern the effective light attenuation length (or light transmission length). This quantity is defined as  $c_{eff}(\lambda) = a(\lambda) + (1 - \langle \cos(\vartheta) \rangle) \cdot b(\lambda)$ , where  $\langle \cos(\vartheta) \rangle$  is the average cosine of the volume scattering function (20).

Water IOPs are wavelength dependent: the light transmission is extremely favoured in the range 350÷550 nm (20) where the photomultipliers used in neutrino telescopes to detect Čerenkov radiation reach the highest quantum

efficiency. In natural seawater, IOPs are also function of water temperature, salinity and dissolved particulate (21; 22). The nature of particulate, either organic or inorganic, its dimension and concentration affect light propagation. All these environmental parameters may vary significantly, for each marine site, as a function of depth and time. It is important, therefore, to perform a long term programme of *in situ* measurements spanning over a long time interval (23). It is known, indeed, that seasonal effects like the increase of surface biological activity (typically during spring) or the precipitation of sediments transported by flooding rivers, enlarge the amount of dissolved and suspended particulate, worsening the water transparency.

We carried out light attenuation and absorption measurements in deep seawater using an experimental set-up based on the AC9. This device performs attenuation and absorption measurements, independently, using two different light paths and spanning the light spectrum over nine different wavelengths (412, 440, 488, 510, 532, 555, 650, 676, 715 nm) (24; 25; 26). The setup designed for deep seawater measurements consists of an AC9, powered by a submersible battery pack, connected to an Idronaut Ocean MK317 CTD (Conductivity, Temperature, Depth) probe. The whole apparatus is mounted inside an AISI-316 stainless-steel cage and it is operated from sea surface down to deep sea, using an electro-mechanical cable mounted on a winch onboard oceanographic research vessels. The same cable is used to transmit the data stream to the ship deck. The DAQ is designed to acquire, about six times per second, water temperature, salinity,  $a(\lambda)$  and  $c(\lambda)$  ( $412 < \lambda < 715$  nm). The apparatus is typically deployed at  $\sim 0.7$  m/s vertical speed, allowing the acquisition of roughly 10 data samples per metre of depth (17; 27). As an example we show in Figure 2 the profiles, as a function of depth, of salinity (in practical salinity units [psu]), temperature ( $^{\circ}\text{C}$ ),  $a(\lambda=440$  nm) and  $c(\lambda=440$  nm) ( $[\text{m}^{-1}]$ ) measured in two deployments at the *KM4* site during December 1999. Each plotted point represents the average value over 10 m depth. The two measurements (red dots and black dots), carried out in two consecutive days, are nearly superimposed. The Figure indicates that deep waters in *KM4* do not show relevant variations of oceanographic and optical properties in the depth interval 2000–3250 m.

### 2.1 AC9 Calibration and systematic errors

As described in previous papers (17; 27), the AC9 measures the difference between the absorption and attenuation coefficients of seawater with respect to the coefficients for pure water. The AC9 manufacturer provides a set of instrument calibration coefficients, that refer to the instrument response to pure water and dry air, used to obtain the absolute values of  $a(\lambda)$  and  $c(\lambda)$ . In order to reduce systematic uncertainties associated to the measurements,

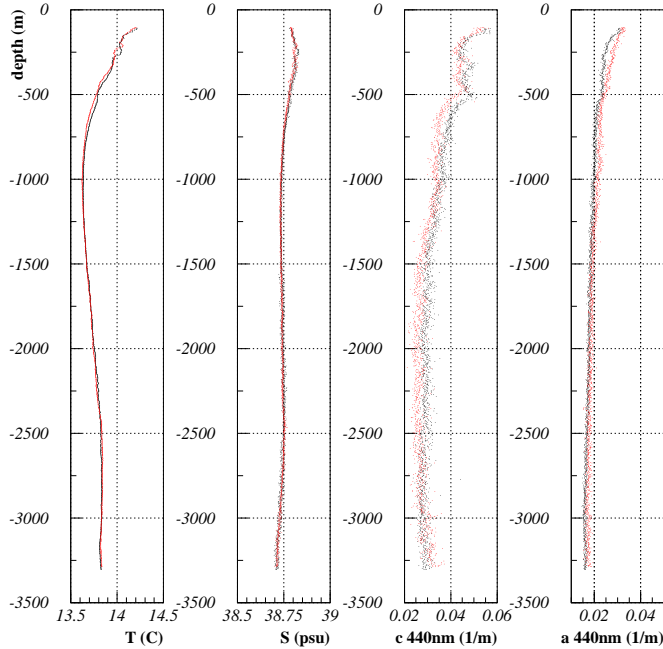


Fig. 2. Temperature [ $^{\circ}\text{C}$ ], salinity [psu], attenuation and absorption coefficients [ $\text{m}^{-1}$ ] for  $\lambda = 440 \text{ nm}$  as a function of depth, measured during two deployments (red and black dots) of the AC9 in *KM4* site in December 1999. Results of the measurements are nearly superimposed.

during each naval campaign, the AC9 calibration coefficients have been verified several times (before and after each deployment), recording the instrument readings for light transmission in high purity grade nitrogen atmosphere. With this calibration procedure we estimated that systematic errors amount to  $\simeq 1.5 \times 10^{-3} \text{ [m}^{-1}\text{]}$  for the  $a(\lambda)$  and  $c(\lambda)$  measurements. We performed in each site at least two deployments of the AC9 setup at short time interval (typically less than 1 day).

### 3 Comparison of deep sea sites in the Central Mediterranean Sea

The first measurements of IOP in *Capo Passero* were carried out in December 1999, in the *KM3* and *KM4* sites. A comparison among the vertical profiles of salinity, temperature,  $a(440 \text{ nm})$  and  $c(440 \text{ nm})$  as a function of depth, recorded in the two sites is shown in Figure 3. Between 1250 m and 3250 m depth, the water column in the site *KM3* shows variations of the attenuation coefficients as a function of depth. We attribute this variation of  $c(\lambda)$  to extra sources of light scattering, due to particulate present in this site, which is close to the Maltese shelf break. We never observed this effect in *KM4*, a site farther from the Maltese Escarpment. Figure 3, indeed, shows that optical properties measured in *KM4* are almost constant as a function of depth (for

depth  $> 1500$  m). Table 1 summarises the values of  $a(\lambda)$  and  $c(\lambda)$ , measured at the *KM3* and *KM4* sites, averaged over an interval of about 400 m depth, 150 m above the seabed ( $\simeq 3400$  m in *KM4*), which is a suitable range for the installation of neutrino telescopes. As explained above two deployments were carried out in each site. Results are reported in the table. During deployments about 10 data acquisitions per metre of depth are recorded, this implies that large statistics is collected with the instrument in a 400 m depth interval allowing to achieve small statistical errors for each absorption or attenuation coefficient. Table 1 does not report the measured values of the  $a(676 \text{ nm})$  coefficient since its value is used in the off-line analysis as a normalization parameter to estimate corrections due to the not perfect reflectivity mirror in the AC9 absorption channel (see reference (17)). During the December 1999 sea campaign, the attenuation channel at  $\lambda=555 \text{ nm}$  was not properly working therefore the  $c(555 \text{ nm})$  value is not given in Table 1.

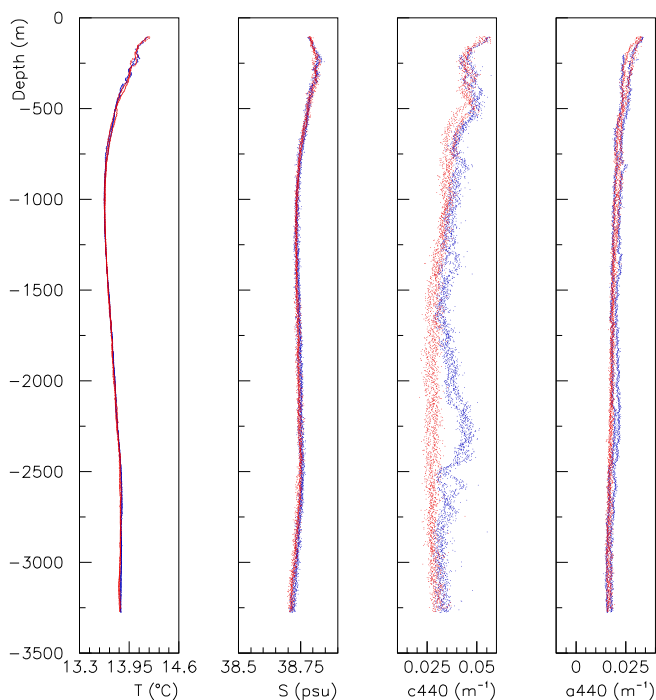


Fig. 3. Comparison between temperature, salinity, attenuation and absorption coefficients (at  $\lambda = 440 \text{ nm}$ ) as a function of depth, measured in *KM4* (red dots) and *KM3* (blue dots) during December 1999. Two deployments were carried out in each site, typically in a time window of 24 hours.

Figure 4 shows the absorption and attenuation lengths ( $L_a(\lambda) = 1/a(\lambda)$ ,  $L_c(\lambda) = 1/c(\lambda)$ ), as a function of the wavelengths (measured in the depth range  $2850 \div 3250$  m) in *Ustica* and *Alicudi* (see reference (17)) and at the *KM3* and *KM4* sites. Data presented for each site are the averages over two



Table 1

December 1999 data. Average values of  $a(\lambda)$  and  $c(\lambda)$  (in units of  $[m^{-1}]$ ) measured in the *KM3* and *KM4* sites, in the depths interval  $2850 \div 3250$  m. The statistical errors are the RMS of the measured distributions. Two deployments were carried out in each site. The systematic errors associated with the absorption coefficient data, in all the following tables, are of the order of  $1.5 \times 10^{-3} [m^{-1}]$ .

coefficient	KM3		KM4	
	1 <sup>st</sup> measurement	2 <sup>nd</sup> measurement	1 <sup>st</sup> measurement	2 <sup>nd</sup> measurement
a412	$0.0168 \pm 0.0006$	$0.0137 \pm 0.0004$	$0.0143 \pm 0.0006$	$0.0149 \pm 0.0008$
a440	$0.0177 \pm 0.0005$	$0.0156 \pm 0.0005$	$0.0159 \pm 0.0005$	$0.0172 \pm 0.0007$
a488	$0.0217 \pm 0.0004$	$0.0209 \pm 0.0004$	$0.0208 \pm 0.0004$	$0.0213 \pm 0.0005$
a510	$0.0370 \pm 0.0004$	$0.0365 \pm 0.0004$	$0.0363 \pm 0.0003$	$0.0374 \pm 0.0005$
a532	$0.0532 \pm 0.0004$	$0.0527 \pm 0.0004$	$0.0528 \pm 0.0003$	$0.0529 \pm 0.0005$
a555	$0.0682 \pm 0.0005$	$0.0683 \pm 0.0005$	$0.0683 \pm 0.0004$	$0.0689 \pm 0.0006$
a650	$0.3557 \pm 0.0003$	$0.3560 \pm 0.0003$	$0.3564 \pm 0.0003$	$0.3581 \pm 0.0003$
a715	$1.0161 \pm 0.0003$	$1.0165 \pm 0.0003$	$1.0167 \pm 0.0003$	$1.0169 \pm 0.0003$
c412	$0.0359 \pm 0.0025$	$0.0336 \pm 0.0022$	$0.0309 \pm 0.0017$	$0.0343 \pm 0.0026$
c440	$0.0335 \pm 0.0024$	$0.0312 \pm 0.0022$	$0.0284 \pm 0.0016$	$0.0292 \pm 0.0025$
c488	$0.0368 \pm 0.0024$	$0.0341 \pm 0.0021$	$0.0309 \pm 0.0015$	$0.0329 \pm 0.0023$
c510	$0.0442 \pm 0.0024$	$0.0417 \pm 0.0020$	$0.0397 \pm 0.0014$	$0.0427 \pm 0.0021$
c532	$0.0546 \pm 0.0024$	$0.0520 \pm 0.0020$	$0.0489 \pm 0.0014$	$0.0514 \pm 0.0020$
c650	$0.3780 \pm 0.0024$	$0.3740 \pm 0.0020$	$0.3719 \pm 0.0016$	$0.3747 \pm 0.0022$
c676	$0.4494 \pm 0.0021$	$0.4508 \pm 0.0018$	$0.4489 \pm 0.0011$	$0.4503 \pm 0.0018$
c715	$1.0209 \pm 0.0020$	$1.0193 \pm 0.0018$	$1.0169 \pm 0.0012$	$1.0190 \pm 0.0018$

deployments; the errors are the RMS of the observed distributions. The same Figure also shows that the values of  $L_a(\lambda)$  and  $L_c(\lambda)$  measured in the region of *Capo Passero* are larger than the ones measured in the other sites. In particular the values of  $L_a(\lambda)$  are comparable to the ones of optically pure seawater quoted by Smith and Baker (28). These results lead us to the conclusion that in *Capo Passero KM4* site the deep seawater optical properties are close to optically pure water ones. Absorption and attenuation coefficients are almost constant for a large interval of depths making this site optimal for the installation of an underwater neutrino telescope. *KM3* site was not considered a valid choice, in spite of the advantage to be closer to the coast, since the measured water optical properties are not constant along the vertical water column: this effect is supposed to be due to the proximity to the shelf break.

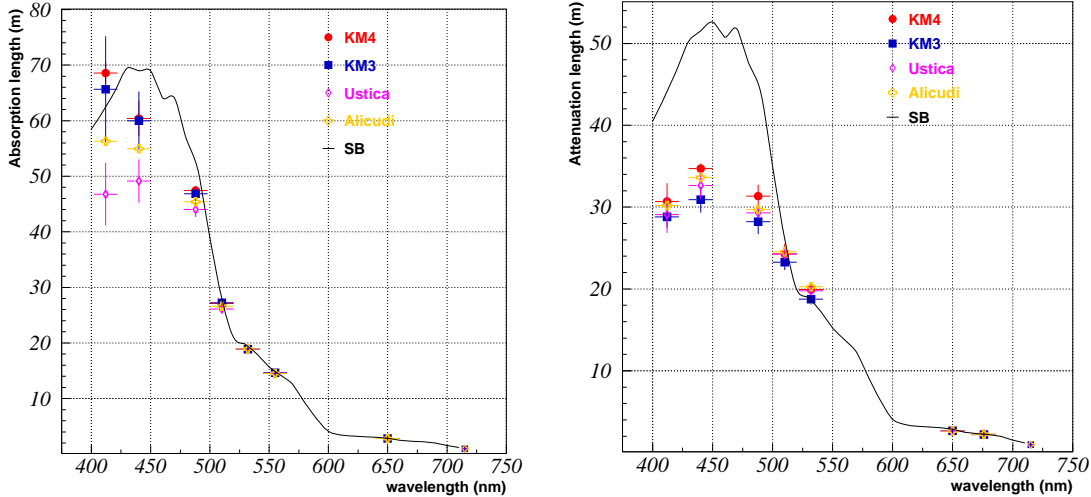


Fig. 4. Average absorption and attenuation lengths measured with the *AC9* in *Ustica*, *Alicudi* ((17)), *Capo Passero* *KM3* and *KM4* sites, in the 2850÷3250 m depth interval. Statistical errors are plotted.  $L_a(\lambda)$  and  $L_c(\lambda)$  of optically pure seawater, reported by Smith and Baker (28), are indicated by a solid black line.

#### 4 Long term study of optical properties at the Capo Passero site

In order to verify the occurrence of seasonal variations of deep seawater IOPs in *KM4*, we are continuously monitoring this site using the experimental setup described above. The data collected during oceanographic campaigns of December 1999, March 2002, May 2002, August 2002 and July 2003 are reported here. In Figure 5 the profiles of water temperature, salinity,  $a(440 \text{ nm})$  and  $c(440 \text{ nm})$ , as a function of depth, are shown. The whole collected data sample consists of: 2 deployments in December 1999 (red dots), 4 deployments in March 2002 (yellow dots), 2 deployments in May 2002 (blue dots), 3 deployments in August 2002 (orange dots), 2 deployments in July 2003 (light blue dots). Seasonal variations are observed only in shallow waters, down to the thermocline depth of about 500 m. At depths greater than 2000 m the  $a(440)$  and  $c(440)$  coefficients measured in different seasons are compatible within the instrument experimental error ( $\Delta T \simeq 10^{-2} \text{ }^\circ\text{C}$ ,  $\Delta S \simeq 10^{-2} \text{ psu}$ ,  $\Delta a, \Delta c \simeq 2.2 \cdot 10^{-3} \text{ m}^{-1}$ ).

Table 2 gives, for each campaign, the weighted average values of the absorption and attenuation coefficients, as a function of wavelength. Weighted average is calculated from the values of  $a(\lambda)$  and  $c(\lambda)$ , measured in each deployment at depths between 2850 and 3250 m. Statistical errors are calculated from the RMS of the observed distributions. In Figure 6 the absorption and attenuation lengths are shown. During December 1999 and March 2002 campaigns the channel  $c(555)$  was not properly working; the same happened to channels  $c(488)$  during all the campaigns after May 2002 and to  $a(488)$  in July 2003.

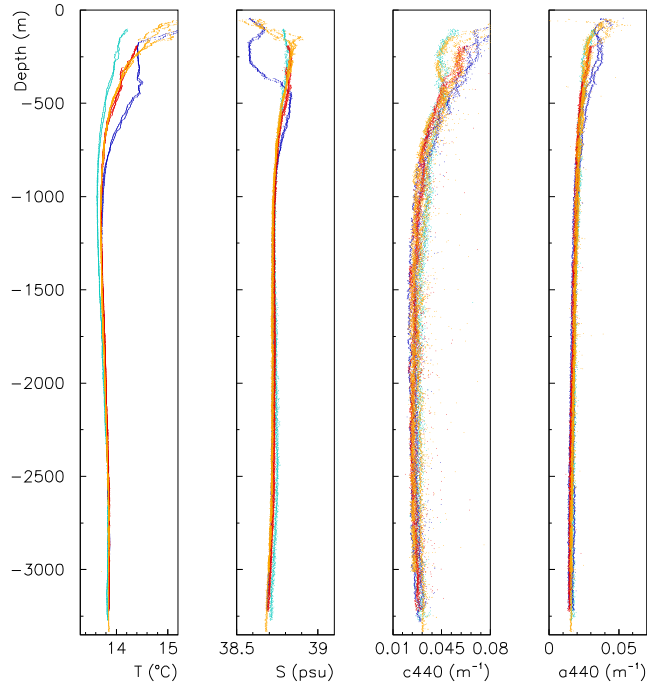


Fig. 5. Profiles of temperature ( $T$ ), salinity ( $S$ ), attenuation coefficient  $c(440 \text{ nm})$  and absorption coefficient  $a(440 \text{ nm})$  measured in the *Capo Passero KM4* site. The profiles refer to the campaigns performed during December 1999 (2 deployments, red dots), March 2002 (4 deployments, yellow dots), May 2002 (2 deployments, blue dots), August 2002 (3 deployments, orange dots) and July 2003 (2 deployments, light blue dots).

The corresponding data are not reported here.

Figure 7 shows the time dependence of the average values of  $L_a(440 \text{ nm})$  and  $L_c(440 \text{ nm})$  as a function of time. The plotted error bars are statistical errors. The average absorption length, calculated using the values of Table 2 weighted with their statistical errors, is  $L_a(\lambda = 440 \text{ nm}) = 66.5 \pm 8.2_{stat} \pm 6.6_{syst}$  m close to the value of optically pure water. The weighted average attenuation length is  $L_c(\lambda = 440 \text{ nm}) = 34.7 \pm 3.3_{stat} \pm 1.8_{syst}$  m close to published values of ocean waters measured in conditions of collimated beam and detector geometry (23). The value of  $L_c$  measured in *Capo Passero* is larger than the one reported by Khanaev and Kuleshov (29) for the NESTOR site. We remind that other results (by DUMAND (30), NESTOR (31) and ANTARES (32)) have been obtained measuring the *effective light attenuation in conditions of not collimated geometry, i.e. using a diffused light source and a large area detector; these results therefore deal with the effective attenuation coefficients and cannot be directly compared with our results.*

Table 2

Weighted average values of  $a(\lambda)$  and  $c(\lambda)$  measured in *Capo Passero KM4* during different seasons, in the interval of depth  $2850 \div 3250$  m.

coefficient	December 1999	March 2002	May 2002	August 2002	July 2003
a412	$0.0145 \pm 0.0008$	$0.0151 \pm 0.0014$	$0.0187 \pm 0.0014$	$0.0205 \pm 0.0008$	$0.0127 \pm 0.0017$
a440	$0.0164 \pm 0.0009$	$0.0166 \pm 0.0011$	$0.0160 \pm 0.0016$	$0.0148 \pm 0.0005$	$0.0126 \pm 0.0010$
a488	$0.0210 \pm 0.0005$	$0.0212 \pm 0.0007$	$0.0189 \pm 0.0013$	$0.0181 \pm 0.0003$	
a510	$0.0366 \pm 0.0007$	$0.0366 \pm 0.0007$	$0.0377 \pm 0.0013$	$0.0383 \pm 0.0005$	$0.0367 \pm 0.0008$
a532	$0.0528 \pm 0.0004$	$0.0529 \pm 0.0006$	$0.0517 \pm 0.0010$	$0.0502 \pm 0.0005$	$0.0507 \pm 0.0006$
a555	$0.0685 \pm 0.0006$	$0.0683 \pm 0.0007$	$0.0675 \pm 0.0008$	$0.0677 \pm 0.0005$	$0.0673 \pm 0.0005$
a650	$0.3572 \pm 0.0009$	$0.3565 \pm 0.0010$	$0.3610 \pm 0.0004$	$0.3619 \pm 0.0004$	$0.3619 \pm 0.0003$
a715	$1.0168 \pm 0.0003$	$1.0117 \pm 0.0014$	$1.0458 \pm 0.0003$	$1.0457 \pm 0.0002$	$1.0451 \pm 0.0003$
c412	$0.0319 \pm 0.0028$	$0.0331 \pm 0.0025$	$0.0351 \pm 0.0033$	$0.0327 \pm 0.0024$	$0.0334 \pm 0.0039$
c440	$0.0287 \pm 0.0021$	$0.0302 \pm 0.0024$	$0.0281 \pm 0.0029$	$0.0283 \pm 0.0023$	$0.0288 \pm 0.0034$
c488	$0.0315 \pm 0.0022$	$0.0329 \pm 0.0027$			
c510	$0.0406 \pm 0.0024$	$0.0414 \pm 0.0022$	$0.0436 \pm 0.0027$	$0.0450 \pm 0.0027$	$0.0459 \pm 0.0027$
c532	$0.0497 \pm 0.0022$	$0.0510 \pm 0.0025$	$0.0577 \pm 0.0016$	$0.0584 \pm 0.0024$	$0.0574 \pm 0.0021$
c555			$0.0808 \pm 0.0029$	$0.0791 \pm 0.0023$	$0.0761 \pm 0.0020$
c650	$0.3729 \pm 0.0024$	$0.3744 \pm 0.0025$	$0.3851 \pm 0.0032$	$0.3849 \pm 0.0034$	$0.3797 \pm 0.0015$
c676	$0.4493 \pm 0.0017$	$0.4502 \pm 0.0015$	$0.4761 \pm 0.0041$	$0.4740 \pm 0.0037$	$0.4684 \pm 0.0022$
c715	$1.0175 \pm 0.0019$	$1.0469 \pm 0.0010$	$1.0645 \pm 0.0032$	$1.0626 \pm 0.0030$	$1.0652 \pm 0.0023$

## 5 Conclusions

The NEMO Collaboration measured, as a function of depth, the salinity, temperature and inherent optical properties in several abyssal sites of the central Mediterranean Sea using an experimental apparatus consisting of an AC9 transmissometer and a standard CTD probe. In order to compare the water transparency to Čerenkov light of different sites we have averaged the measured values of  $c(\lambda)$  and  $a(\lambda)$  in a range of about 400 m, at the depths which are suitable for the deployment of a  $\text{km}^3$  neutrino telescope. The data of  $L_a(\lambda)$  presented for *Capo Passero KM4* site are close to the ones reported by Smith and Baker for optically pure seawater (28). For blue light, the average absorption length is  $\simeq 67$  m, the average attenuation length is  $\simeq 35$  m. It is worth to mention that all the measurements reported in this paper have been carried out over an area of about  $10 \text{ km}^2$  around the reference point of *KM4*. We conclude that optical and oceanographic properties in *Capo Passero KM4* site are ho-

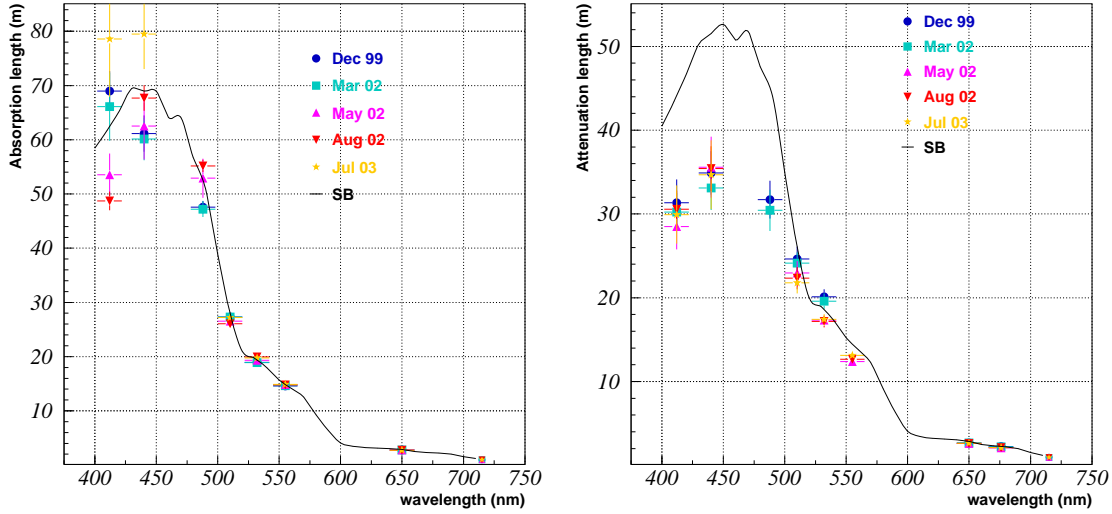


Fig. 6. Average absorption and attenuation lengths measured with the *AC9* in *KM4*, at depth  $2850 \div 3250$  m in December 1999 (blue circle), March 2002 (light blue square), May 2002 (purple triangle), August 2002 (red upsidedown triangle) and July 2003 (dark yellow star). Statistical errors are plotted. A solid black line indicates the values of  $L_a(\lambda)$  and  $L_c(\lambda)$  for optically pure seawater reported by Smith and Baker (28).

*mogeneous in a large region and constant over the investigated timescale. The measured absolute values of IOP and the homogeneity of the water column, for more than one thousand metres above the seabed, make Capo Passero KM4 an optimal site for the installation of the future Mediterranean km<sup>3</sup> underwater neutrino telescope.*

## 6 Acknowledgements

*This work has been conducted in collaboration with: Department of Physical Oceanography INOGS (Trieste), Istituto Sperimentale Talassografico CNR (Messina) and Istituto di Oceanografia Fisica CNR (La Spezia). We thank Captains E. Gentile, V. Lubrano, A. Patané, the officers and the crew of the R/V Alliance, Thetis and Urania for their outstanding experience shown during the sea campaigns.*

## References

- [1] T.K. Gaisser, F. Halzen and T. Stanev, *Phys. Rep.* **258**, 173 (1995).
- [2] J. Learned and K. Mannheim, *Ann. Rev. Nuc. Part. Sci.* **50**, 679 (2000).
- [3] K. Mannheim, *Astron. and Astrophys* **3**, 295 (1995).

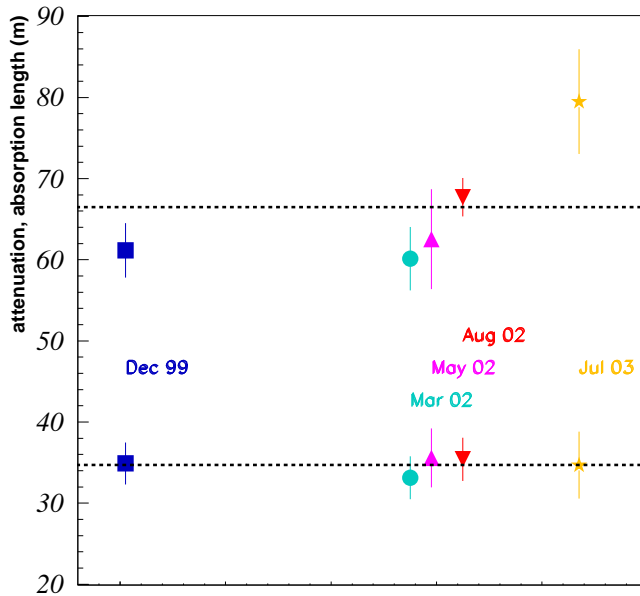


Fig. 7. Average attenuation and absorption lengths at  $\lambda=440$  nm measured with the *AC9* in *KM4*, at depth  $2850\div 3250$  m in December 1999 (blue circle), March 2002 (light blue square), May 2002 (purple triangle), August 2002 (red upsidedown triangle) and July 2003 (dark yellow star). The weighted average values of  $L_a(440)$  and  $L_c(440)$  are indicated by dashed black lines (see text). Statistical errors are shown.

- [4] *R. Protheroe et al*, *Astropart. Phys.* **9**, 1 (1998).
- [5] *C. Distefano et al*, *Astrophys. J.* **575**, 378 (2002).
- [6] *E. Waxmann and J. Bahcall*, *Phys. Rev. Lett.* **78**, 2292 (1997).
- [7] *M.A. Markov and I.M. Zheleznykh*, *Nucl. Phys.* **27**, 385 (1961).
- [8] *J. Aahrens et al*, *Phys. Rev. Lett.* **90**, 251101 (2003).
- [9] *V. Ayutdinov et al.*, *Proc. of the 28th International Cosmic Ray Conference, Tsukuba, Japan (2003)*.
- [10] <http://amanda.berkeley.edu>.
- [11] <http://icecube.wisc.edu>.
- [12] <http://desy.ifh.de/>.
- [13] <http://www.nestor.org.gr>.
- [14] <http://antares.in2p3.fr>.
- [15] <http://nemoweb.lns.infn.it>.
- [16] *G. Riccobene for the NEMO Collaboration*, *Proc. of the Workshop on methodical aspects for underwater neutrino telescopes, Hamburg, Germany (2001)*.
- [17] *A. Capone et al.*, *Nucl. Instr. Meth.* **A487** 423 (2002).
- [18] *NEMO Collaboration*, *Study and characterization of a deep sea site for a  $km^3$  underwater neutrino telescope*, Report to ApPEC Peer Review Committee, (2003), <http://nemoweb.lns.infn.it/sites/sitereport>.
- [19] <http://www.wetlabs.com>.

- [20] *C.D. Mobley, Light and Water, Academic Press, San Diego (1994).*
- [21] *R.M. Pope and E.S. Fry, Applied Optics **36** 33 (1997).*
- [22] *L. Kou, D. Labrie and P. Chylek Applied Optics **32** 3531 (1993).*
- [23] *S.Q. Duntley, J. Opt. Soc. Am. **53** 214 (1963).*
- [24] *M.S. Twardowski et al., J. of Atm. and Ocean. Tech. **16** 691 (1999).*
- [25] *J.R.V. Zaneveld and J.C. Kitchen, SPIE Vol. 2258 Ocean Optics XII, **49** (1994).*
- [26] *W.S. Pegau, D. Gray and J.R.V. Zaneveld, Applied Optics **36** 6035 (1997).*
- [27] *V. Balkanov et al., Nucl. Instr. Meth. **A489** 231 (2003) .*
- [28] *R.C. Smith and K.S. Baker, Applied Optics **20** 177 (1981).*
- [29] *S.A. Kanaev and A.P. Kuleshov, Proceedings of the 3<sup>rd</sup> NESTOR Workshop, Pylos (1983).*
- [30] *H. Bradner and G. Blackinton, Applied Optics **23** 1009 (1984).*
- [31] *E.G. Anassontzis et al., Nucl. Inst. Met. **A349** 242 (1994).*
- [32] *J.A. Aguilar et al., Astropart. Phys. **23** (2005) 131.*